Liu Yunyun (Orcid ID: 0000-0003-0217-0591)

Was the Extremely Wet Winter of 2018/19 in the Lower Reach of the Yangtze River Driven by ENSO?

Yunyun Liu[1, 2], Zeng-Zhen Hu[3], and Renguang Wu[4]

(1) Laboratory of Climate studies, National Climate Center, China Meteorological Administration, Beijing 100081, China

(2) Collaborative Innovation Center on Forecast and Evaluation of Meteorological Disasters, Nanjing University of Information Sciences & Technology, Nanjing 210044, China

(3) Climate Prediction Center, NCEP/NOAA, College Park, MD 20740, USA

(4) School of Earth Sciences, Zhejiang University, Hangzhou, Zhejiang 310027, China

*Corresponding author address:

Yunyun Liu

National Climate Center

Chinese Meteorological Administration

#46 Zhong-Guan-Cun South Road

This is the author manuscript accepted for publication and has undergone full peer review but has not been through the copyediting, typesetting, pagination and proofreading process, which may lead to differences between this version and the Version of Record. Please cite this article as doi: 10.1002/joc.6591

Beijing 100081, China

liuyuny@cma.gov.cn

Abstract

In the winter of 2018/19, the lower reach of the Yangtze River (LRYR) of China experienced an excessive amount of precipitation with a long duration. Such an extreme event occurred in the mature phase of an El Niño under the background of global warming, and thus, attracted great attention in the society and climate community. Presumably, this extreme event was driven by the El Niño.

In this work, based on observational diagnoses and real-time model forecasts, we investigate the contributions of oceanic forcing and the predictability of this event. It is argued that tropical Atlantic warming, interdecadal variation, and central tropical Pacific warming (associated with central Pacific instead of eastern Pacific El Niño) are three major factors leading to the extreme event. In addition to the recognized impact from sea surface temperature anomalies (SSTAs) associated with central Pacific El Niño, tropical Atlantic warming makes an important contribution to the Atlantic-Eurasian circulation change through a global zonal wave pattern extending from the tropical Atlantic to East Asia. Moreover, a climate model successfully predicted the wet pattern in LRYR in short (1-5 month) lead real-time predictions, and captured the observed statistical relationship between the winter precipitation in LRYR and the SSTA in the central tropical Pacific and equatorial Atlantic Oceans. These results indicate that such an event is predictable to some extent.

Keywords： Extremely wet winter of 2018/19; Lower reach of the Yangtze River; Central Pacific El Niño; Tropical Atlantic warming; Interdecadal variation; Predictability

1. Introduction

Southern China (SC, the blue rectangle in Fig.1a) is a region of a large population and constitutes a large economic zone. In this region, the precipitation exhibits a large interannual variability not only in summer but also in winter, and the precipitation-related climate extreme events can result in a huge social and economic damage. In winter 2018/19, SC experienced exceptionally excessive and sustained precipitation anomaly, with the maximum center in the lower reach of the Yangtze River (LRYR, the red rectangle of Fig. 1a). The precipitation in most areas of LRYR was greater than two standard deviations and the precipitation days even exceeded three standard deviations, setting a record of the largest precipitation amount and the longest duration since 1951 (Figs. 1, 2). This extremely wet winter event had a great impact on transportation, agriculture, and people's life in SC.

Persistent drought and flood are usually the results of some persistent atmospheric circulation anomalies (Tao et al., 1962; Zhang et al., 2008) that, in turn, may be related to external forcings, such as sea surface temperature (SST), snow cover, etc. Because of the wide area and large heat capacity, the state of ocean is especially valued by meteorologists (e.g., Zhang et al., 1996; Wang et al., 2000; Zhang and Sumi, 2002; Xie et al., 2009; Liu et al., 2012; 2013, 2014; Wang and Chen, 2014; Xu et al., 2019, Hu et al. 2020). Previous studies indicated that the El Niño-Southern Oscillation (ENSO) is one of the most important factors to the precipitation variability in SC (Lau and Nath, 2003; Wu et al., 2003; Chang et al., 2004; He and Wang, 2013). Winter (December-January-February, DJF) precipitation

in SC tends to be above normal during the mature phase of an El Niño event (Zhang et al., 1999; Zhang and Sumi, 2002; Wu et al., 2003; Yuan et al., 2014). However, different flavors of El Niño may have different impacts on the precipitation anomaly in SC (Feng et al., 2010; Feng and Li, 2011; Hu et al., 2012; Yuan and Yang, 2012; Xu et al., 2019). It was suggested that the precipitation anomaly in SC is statistically larger during the mature phase of eastern Pacific (EP) El Niño than that of central Pacific (CP) El Niño. Geographically, compared with EP El Niño, the maximum wet center shifts northward from the southeast coast of SC to LRYR (Fig. 1a) in CP El Niño (Su et al., 2013). The different precipitation distributions over SC in EP and CP El Niño are attributed to the differences in anomalous Walker circulation and low-level anticyclone around the Philippines. Both the Philippine anticyclone and the descending branch center of the Walker circulation over the western North Pacific occupy a smaller domain and are located more northward during CP El Niño than during EP El Niño (Feng et al., 2010).

In addition to the effects of ENSO, the winter precipitation anomalies in SC may be affected by other external forcing factors, such as the SST anomalies (SSTAs) in the tropical western Indian Ocean (Liu et al., 2010), in the North Atlantic Ocean (Li et al., 2007; Fu et al., 2008; Han et al., 2011), in the Kuroshio Sea (Zong et al., 2008; Liu et al., 2010), as well as convective activities in the equatorial central and western Pacific Ocean (Nitta and Hu, 1996; Guo et al., 1998). These external forcings affect the precipitation anomalies in SC through modifying the geopotential height and wind fields in the upper and lower troposphere over the Asian region (Zhang et al., 2008;

Liu et al., 2013). On the other hand, both the winter precipitation and its interannual variability in SC have experienced significant interdecadal change during the end of the 1980s (Zhang et al., 2008; Qian, 2013; Zhang et al., 2018), which may also contribute to the extremely wet winter event in 2018/19.

Co-occurrence with the extremely wet winter event in LRYR, the SST warming was observed in the equatorial central and eastern Pacific, forming an El Niño event in winter 2018/19. A question is whether this extremely wet winter event in LRYR was driven by canonical ENSO? Meanwhile, the observed SST in the tropical Indian Ocean and the equatorial Atlantic Ocean was also abnormally high, with the highest equatorial Atlantic Niño SST index (ATL3, Zebiak, 1993) since 1951. Are there contributions of SSTAs in the tropical Indian and Atlantic Oceans to the extremely wet winter in LRYR as well? As for the impact of the equatorial Atlantic Ocean, previous studies suggest that the tropical Atlantic Ocean plays an important role in the climate variability in the Atlantic European sector in boreal winter based on observations (e.g., Czaja and Frankignoul, 2002) and model studies (e.g., Drevillon et al., 2003, Mathieu et al., 2004). These previous studies, however, did not deal with the impact of equatorial Atlantic SSTA on winter climatic anomalies in East Asia.

The purpose of this study is to investigate possible factors leading to the extremely wet winter of 2018/19 in LRYR and its predictability. We focus on the following two objectives: (1) What are the roles of ENSO and the Indian and Atlantic Oceans and the contribution of interdecadal variation of precipitation? (2) What is the predictability of this event and what fraction is predictable? The remainder of the

paper is organized as follows. Section 2 provides a description of the datasets and models used in this study. The characteristics, possible factors, and predictability of the extreme event are addressed in sections 3 and 4. Section 5 is a summary and discussion.

2. Data, SSTA indices, and models

The main datasets utilized in this work include precipitation from 700 representative stations in China from Jan 1951 to Feb 2019 provided by the China Meteorological Administration, NOAA's PRECipitation REConstruction Dataset (Chen et al., 2002), and the US National Centers for Environmental Prediction/National Center for Atmospheric Research (NCEP/NCAR) reanalysis products (Kalnay et al., 1996), including monthly mean 200 hPa geopotential height (Z200) and stream function (S200). Monthly mean SST on a 2°× 2° resolution is extracted from the National Oceanic and Atmospheric Administration Extended Reconstructed SST, version 5 (ERSSTv5; Huang et al., 2017). The present study focuses on the winter (DJF) season covering the 1951/52-2018/19 period. Anomalies of all variables are defined as the deviations from the climatological mean of DJF for the period 1981/82-2010/11. Linear correlation and regression are used in this study. The statistical significance of the correlation is estimated using the two-tailed Student's *t*-test. For the winters of 1951/52-2018/19, the correlation coefficients at the confidence levels of 90%, 95%, and 99% are 0.20, 0.24 and 0.31, respectively.

To measure the tropical SSTA variations and their association with the

atmosphere, different SSTA indices are selected in this work. In addition to the Niño3.4 index, Cold Tongue (CT) and Warm Pool (WP) (Kug et al., 2009; Ren and Jin, 2011) and Modoki (Ashok et al., 2007) indices are used to represent different flavors of ENSO. There are two main SSTA patterns in the tropical Indian Ocean: the Indian Ocean dipole mode (IOD, Saji et al., 1999) and the Indian Ocean basin mode (IOBM, Chambers et al., 1999). The equatorial Atlantic Niño (ATL3, Zebiak, 1993) and tropical North Atlantic (TNA, Enfield et al., 1999) indices are two indices to represent the SSTA in the Atlantic Ocean. The linear trends of these SST indices have been removed first when calculating the correlation and reconstruction of precipitation anomaly in LRYR using these SST indices. The definitions of these SSTA indices are as follows:

(1) Niño3.4 = SSTA (5°S-5°N, 170°-120°W);

(2) CT = $SSTA_{Niño3}$ (5°S-5°N, 150°-90°W) - α*$SSTA_{Niño4}$ (5°S-5°N, 160°E-150°W),

(3) WP = $SSTA_{Niño4}$ (5°S-5°N, 160°E-150°W) - α*$SSTA_{Niño3}$ (5°S-5°N, 150°-90°W), (while $SSTA_{Niño3}$*$SSTA_{Niño4}$ >0, α = 0.4; otherwise, α = 0);

(4) Modoki = SSTA (10°S-10°N, 165°-140°W) – [SSTA (15°S-5°N, 110°-70°W) + SSTA (10°S-20°N, 125°-145°E)]/2;

(5) IOBM = SSTA (20°S-20°N, 40°-110°E);

(6) IOD = SSTA (10°S-10°N, 50°-70°E) - SSTA (10°S-0°, 90°-110°E);

(7) ATL3 = SSTA (3°S-3°N, 20°W-0°);

(8) TNA = SSTA (5.5°-23.5°N, 57.5°-15°W).

Also, ensemble means of hindcasts and real-time predictions initiated from

January 1982-December 2018 from the NCEP Climate Forecast System version 2 (CFSv2) are examined in this work to investigate the predictability of this event and the statistical connection with SSTAs (Xue et al., 2013; Saha et al., 2014; Hu et al., 2013; 2014; 2017). The ensemble means of the real-time predictions include 40 members within the last 10 days of each month and four forecasts per day, out to 9 months.

3. Wet Winter of 2018/19 in LRYR and Associated Atmospheric and Oceanic Anomalies

Climatologically, precipitation amount in winter generally decreases from south to north over China, and SC has the most abundant precipitation, with the climate mean of 100-280 mm in DJF (Figure not shown). In winter 2018/19, precipitation in DJF was 100-200 mm above the climate mean in most areas of LRYR, greater than two standard deviations (Fig. 1a). Furthermore, the number of precipitation days was generally 30-60 days in most of the LRYR region, about 15 days more than the climate mean, exceeding three standard deviations (Fig. 1b). The wet winter of 2018/19 in LRYR was characterized as the largest precipitation and the longest duration since 1951/52 winter (Fig. 2). On the other hand, the excessive precipitation did not occur in the entire SC, and there were deficit precipitation and less number of precipitation days than normal in the southeastern coast of SC.

The contemporary upper-level atmospheric circulation anomalies in DJF 2018/19 are shown in Fig. 3. Globally, there is a zonal wave train in the subtropical and

mid-latitudes from the North Atlantic to East Asia (Fig. 3a). Locally, an anomalous anticyclone is present over the South China Sea (SCS)-eastern coast of China, and an anomalous cyclone lies to its western side. As low-frequency height anomalies in extratropics are of barotropic vertical structure (Wallace and Blackmon, 1983), the local circulation anomalies are accompanied by strong southerly surface wind anomalies over East China, which brought abundant water vapor and excessive precipitation over LRYR in winter 2018/19 (Fig. 1).

For the ocean conditions, SSTs were above normal across the central and eastern equatorial Pacific during DJF 2018/19 (Fig. 3a). The Niño3.4, CT, WP, and Modoki indices are 0.79, 0.35, 0.64 and 0.44 in DJF 2018/19, respectively. According to the definition of Ren and Jin (2011), this 2018/19 ENSO event is a CP or CP/EP mixed type El Niño as the WP index is larger than the CT index. Tropical SST anomalies are usually expected to be a forcing for the global atmosphere, and such a large amplitude of extra-tropical height anomalies (Fig. 3a), if indeed a forced response to SSTs, usually only be expected during a strong El Nino winter (Kumar and Hoerling, 1997). And thus, in addition to the weak El Niño evernt in winter 2018/19, other factors may also contribute to the extreme event in SC.

It is noted that that the positive SSTA is present in the equatorial Atlantic Ocean and there is slightly below-normal SST to the north (Fig. 3a). The ATL3 and TNA indices are 0.65 and -0.02 in DJF 2018/19, respectively. Especially, the ATL3 index is the strongest since 1951 (Fig. 2). Meanwhile, positive SSTA is present in the entire basin of the tropical Indian Ocean with SSTA larger in the west than in the east (Fig.

3a). Both the IOBM and IOD indices are positive, with the values of 0.38 and 0.18 in DJF 2018/19, respectively.

The effect of tropical SST forcing can be better assessed by examing the heating-circulation pattern relationship in the tropics (Peng et al., 2018; 2019). Figure 3b presents the DJF S200 and Precipitation anomalies. The reason for using S200 instead of Z200 is that it better depicts atmosphere circulation and waves in the tropics (as the geostropical relationship between wind and height is not well defined over low latitudes). The precipitation anomalies (latent heating) in the tropical Pacific have a positive-negative dipole structure, with positive anomaly (heating) centered near the Dateline and the negative anomaly (cooling) in the eastern Pacific. Similarly, the positive precipitation anomaly (heating) is seen in the equatorial western Atlantic Ocean. Such distributions of precipitation anomaly are consistent with SST anomalies.

According to previous studies of circulation response to tropical forcing (Gill, 1980; Sardeshumkh and Hoskins, 1988; Hoerling et al., 1992; Ting and Hoerlingng, 1993; Alexander et al., 2002), the upper-tropospheric response to equatorial heating has its strongest signal in the tropics (when stream function is used to represent atmospheric circulations), which appears as twin anticyclones (cyclone) symmetrical with respect to the equator and centered at around 15 degrees North and South respectively, and straddling the heating (cooling) pattern (e.g., Fig. 4 in Alexander et al., 2002). This kind of tropical heating-circulation response pattern is apparent in both the tropical central Pacific and Atlantic Oceans. Thus, the warming in the

tropical central Pacific and tropical Atlantic Oceans may be potential contributors to the winter extreme in LRYR in 2018/19.

Figure 3b also shows the wave activity flux (WAF) vectors. It is a useful diagnostic tool for examining the energy dispersion characteristics associated with a Rossby wave train (Plumb 1985; Takaya and Nakamura, 2001; Wu et al., 2003; Tam and Li, 2006). It is noted that the globally zonal wave train in the subtropical and mid-latitudes originates from the tropical Atlantic Ocean and propagates northward to southwestern coast of Europe, and then turned southeastward to the Arabian Peninsula, and arriving via Tibet Plateau to eastern coast of China where it bifurcated, with one branch turning to the south and ending at the tropical central Pacific, and the other branch continuing to go eastward and reaching western North America, where it further turned southeastward and finally diminished over northern tropical Atlantic. It indicates the contribution of the equatorial Atlantic warming to the globally zonal wave train genesis. Thus, SSTAs in tropical regions are potential factors leading to precipitation anomaly in LRYR in winter 2018/19.

4. Predictability of the extremely wet winter in LRYR

4.1 Correlation with different SSTA indices

The extremely wet winter in LRYR in 2018/19 occurred in the mature phase of a weak El Niño event. Previous works have indicated that SC tends to experience a weaker-than-normal East Asian winter monsoon and an overall wetter condition in winter during the mature phase of El Niño year (Wu et al., 2003; Yuan and Yang, 2012;

Yuan et al., 2014). To further check the contributions of ENSO and tropical SSTAs in other oceans, and the predictability of this event, the statistical relations between various tropical SSTA indices and winter precipitation from 1951/52 to 2018/19 are examined first (Table 1, Fig. 4).

According to the correlation coefficients between the time series of precipitation anomaly averaged inLRYR and various tropical SSTA indices, the winter precipitation anomaly in LRYR may be related to ENSO, the Indian Ocean basin mode, and the equatorial Atlantic Niño (Table 1). In the spatial correlation distributions (Fig. 4), however, both the Niño3.4 and CT indices have a significantly positive correlation with the winter precipitation in SC, with the maximum correlation center located on the southeastern coast of China instead of LRYR (Fig. 4a, b), with significantly correlated of these two indices (Table 1). This is consistent with previous studies, indicative of the typical influence of EP ENSO (Wu et al., 2003; Yuan and Yang, 2012). Also, the correlation of IOBM with the winter precipitation is similar to that of Niño3.4 and CT with positive correlations in the entire SC region (Fig. 4e), which is different from the spatial distribution of precipitation anomaly in winter 2018/19 (Fig. 1). Neither IOD nor TNA has a significant correlation with the precipitation in LRYR (Fig. 4f, h). Thus, SSTAs in the eastern tropical Pacific, Indian and tropical North Atlantic Oceans are not the major factors leading to the extremely wet winter in LRYR in 2018/19.

Unlike the spatial correlation with the Niño3.4 and CT indices (Fig. 4a, b), significant correlation regions with both the WP and Modoki indices are mainly

located in the middle and lower reaches of the Yangtze River (Fig. 4c, d), geographically similar to the observed precipitation anomaly pattern in DJF 2018/19 (Fig. 1). Su et al. (2013) found similar results about the different impacts of two types of El Niño on the winter precipitation through composite analysis and model simulation. The high similarity between Fig. 4c and 4d is due to the high correlation between the two indices though the correlation of the WP index is more similar to the spataial distribution of observation than that of El Niño Modoki. Interestingly and notably, the spatial pattern of the correlation with ATL3 (Fig. 4g) is also similar to the observed precipitation anomaly pattern in DJF 2018/19 (Fig. 1). Moreover, the ATL3 index has no significant simultaneous correlations with any ENSO-related indices used in this work (Table 1). Therefore, based on the comparison of the correlation pattern with the observed winter precipitation anomaly in 2018/19, it confirms that the warming in the tropical central Pacific and tropical Atlantic Oceans may be potential contributors to the winter extreme in LRYR in 2018/19, although the correlation coefficients of the two factors are not the most significant (Table 1).

4.2 Reconstruction of the winter precipitation of 2018/19

To further quantify the contributions of warming in the tropical central Pacific and equatorial Atlantic Oceans to the winter extreme in 2018/19, we use the linear regression method to reconstruct the winter precipitation anomaly in LRYR in DJF 2018/19. Firstly, the winter precipitation anomalies at each station are regressed onto the de-trended WP and ATL3 indices. Then, the linear regression coefficients are

multiplied by corresponding values of each of the two indices in DJF 2018/19 to reconstruct precipitation anomalies in winter 2018/19. The observed distribution of excessive precipitation in LRYR and deficit precipitation in the coastal areas of SC are well reproduced by either the WP or ATL3 (Fig. 5a, b). Nevertheless, the reconstructed precipitation anomaly based on either WP or ATL3 is only about 1/4 of the observed precipitation anomaly in DJF 2018/19, implying that other factors contribute to the precipitation anomaly in LRYR in DJF 2018/19.

Interdecadal variation is another contributor to the precipitation anomaly in LRYR in DJF 2018/19. According to the moving *t*-test result of precipitation time series, there is an indication that the winter 1988/89 is a significant interdecadal turning point (Fig. 6), and the winter precipitation in LRYR has increased since the end of the 1980s. It is consistent with previous studies (Zhang et al., 2008; Qian, 2013; Zhang et al., 2018). Zhang et al. (2008) used a longer time series (1880~2008) to analyze the characteristics of precipitation anomaly in SC and found that the end of the 1980s is one of the interdecadal turning points, with no obvious long-term trend. Zhou et al. (2010, 2011) indicated that the strength of East Asian winter monsoon (EAWM) has a significant effect on the winter precipitation anomaly in SC, i.e., the stronger EAWM tends to lead to less precipitation and the weaker EAWM tends to lead to more precipitation. Both the interdecadal variation of the East Asian monsoon circulation itself (Wang, 2001; Kimoto, 2005; Shi et al., 2007; Liu et al., 2013) and the interdecadal variation of the relationship between the EAWM and ENSO (Yuan et al., 2014; Zhang et al. 2018) jointly led to the obvious difference of winter

precipitation in SC at the end of 1980s.

The winter precipitation in LRYR (Fig. 2) is a deficit in 1951/52-1988/89, with an average value of 180 mm, and it is an abundance in 1989/90-2018/19, with an average value of 218 mm. The difference between the two periods is 38 mm, which is 19% higher than the climatic mean of 200 mm. The spatial distribution (Fig. 5c) shows that the winter precipitation in LRYR has distinctly increased during the last 30 years, with the maximum center in LRYR reaching 60 mm. The increment is comparable to the precipitation anomaly reconstructed based on either WP or ATL3 (Fig. 5a, b).

Thus, from the statistical correlations and the reconstructions, it is concluded that the SSTA in the central tropical Pacific Ocean associated with CP El Niño, contributed to the observed precipitation anomaly in LRYR in DJF 2018/19. And the warming in the equatorial Atlantic Oceans and the interdecadal change are additional key players leading to the winter wet extreme in LRYR in 2018/19 (Fig. 5d). Such ocean forcing and long-term variation may imply predictability of this extreme event.

4.3 Mechanisms of the warming in the central tropical Pacific and equatorial Atlantic Oceans

There have been studies on the mechanism of ENSO's influence on winter precipitation in SC. The response of SC precipitation to ENSO is usually attributed to anomalous Walker circulation and the associated anomalous anticyclone-cyclone around the Philippines (Wang et al., 2000, Chang et al., 2004). During CP El Niño

episodes, the Philippine Sea anomalous anticyclone and related anomalous descending shift northwestward to SCS compared to EP El Niño, with relatively weak intensity (Fig. 7e), causing the northward shift of the positive precipitation anomaly center from the southeast coast of SC to LRYR (Feng et al., 2010; Su et al., 2013; Xu et al., 2019). That is consistent with the observed circulation anomalies and the spatial distribution of precipitation anomalies in DJF 2018/19 (Figs.1, 3). However, the observed anomalies in DJF 2018/19 have some differences compared with the statistical relations indicated in the previous studies, such as the intensity of the precipitation anomaly and the position of the Philippine Sea anticyclone anomaly. It implies that only ENSO cannot fully explain the extremely wet winter in DJF 2018/19. Remote influence of the equatorial Atlantic SSTA is an additional potential factor affecting winter precipitation in the LRYR region.

What is the mechanism conveying the remote influences of the equatorial Atlantic SSTA to LRYR region and affecting local precipitation? To investigate the impact of the equatorial Atlantic warming on the precipitation in LRYR, Fig. 7 presents the composite fields in the typical anomalous ATL3 years similar to Fig. 3. Taking one standard deviation of the de-trended ATL3 index as the criteria, seven positive winters of 1981/82, 1987/88, 1997/1998, 2003/04, 2008/09, 2010 /11, and 2018/19 and five negative winters of 1991/92, 1996/97, 2001/02, 2011/12, and 2013/14 are selected to make the composite fields. The obtained composite fields further confirm the possible influence of the tropical Atlantic warming (Fig. 7). There are obvious positive SSTA in the equatorial Atlantic and relatively weak SSTA in

other tropical Oceans (Fig. 7a). A zonal wave train from the tropical Atlantic to the mid-latitudes of East Asia is captured to some extent in the upper troposphere though there is a slight deviation in the position of anomalous centers compared with that in winter 2018/19 (Fig. 3a). It is implied that anomalous warming in the tropical Atlantic Ocean can generate anomalous circulation in the mid-latitude region and affects precipitation anomaly over eastern China. Further, the composite tropical precipitation, S200 and associated WAF in the anomalous ATL3 winters are investigated for the connection of the zonal wave train pattern with the equatorial Atlantic warming (Fig. 7b). Distributions of precipitation and S200 anomalies are similar to those in winter 2018/19, and the wave activity fluxes from northern tropical Atlantic to East Asia support the effect of ATL3 warming by the wave train.

Through the statistical analysis, it is noted that the extremely wet winter in DJF 2018/19 was due to not only the contribution of CP El Niño, but also the contribution of the equatorial Atlantic warming with different influence mechanisms.

4.4 CFSv2 real-time prediction

The statistical connections of SSTAs in the tropical Pacific and Atlantic Oceans with winter climate variability in LRYR discussed in previous subsections imply predictability that are supported by the evidence of relative high prediction skill of CFSv2 (Fig. 8). From Fig. 8, it is noted that the highest prediction skill of winter precipitation variability in the region is in the south of the middle and low reaches of the Yangtze River. The skill is still moderate even in 5-6 month lead prediction (Fig.

8c, d).

The predictability and possible connection of SSTAs with the extreme precipitation event are further examined by the real-time forecasts of CFSv2 (Fig. 9). A comparison of the predictions at different leading times shows that the characteristics of the wet anomaly in LRYR in the winter of 2018/19 is well captured in the short lead predictions. In the 1-month lead (Fig. 9a), both the pattern and amplitude of the precipitation anomaly are well predicted. The maximum center in LRYR exceeds 100 mm in winter. However, the predicted anomaly amplitude declines significantly in the 3-month and 5-month lead prediction though a similar anomaly pattern is predicted (Fig. 9b, c). For the 7-month lead (Fig. 9d), the predicted anomalies are opposite to the observed ones. The decline of the prediction ability with the lead-time increase is due to the accumulation of model biases and also associated with the decrease of the ability in capturing the external forcing (SSTA) with lead-time increase.

For the predicted DJF precipitation averaged in LRYR, it is seen that predicted precipitation anomaly in DJF 2018/19 is about one standard deviation for 1-month lead (Fig. 10a), about a half of standard deviation for 3- and 5-month lead (Fig. 10b, c), and became negative for 7-month lead (Fig. 10d), consisting with the results shown in Fig. 9. Such results suggest that although the predictions at a short lead time (such as less than 5 months) are qualitively correct for the precipitation anomaly in LRYR in DJF 2018/19, predicted precipitation anomaly amplitude is far blow the observation. That implies a challenge for climate models in quantantively predicting a

extreme event, such as DJF 2018/19.

Considering that the winter precipitation anomaly over LRYR is closely related to the SSTA in the tropical Pacific and Atlantic Oceans according to the above analysis, Figure 11 shows the predicted SSTA in winter at different leading times. As the predicted precipitation, the observed SSTAs in the tropical oceans are well captured in the short lead predictions (Fig. 3a). In the 1-month lead (Fig. 11a), the positive SSTAs are well predicted in both the equatorial central and eastern Pacific and tropical Atlantic Oceans. In the 3-month lead (Fig. 11b), the amplitude of predicted SSTA becomes stronger in the eastern Pacific and weaker in the tropical Atlantic, which corresponds to the weaker precipitation anomaly in the prediction (Fig. 9b). With the increase of lead time, the positive SSTA decreases obviously in both the tropical Pacific and Atlantic Oceans, and the cold SSTA occurs in the equatorial Atlantic in the 5-month and 7-month leads (Fig. 11c, d). It may imply that the prediction ability of SST in the CFSv2 model is crucial for the predictability of precipitation in East Asia.

Figure 12 shows the simultaneous correlations of the precipitation anomaly in LRYR and SSTA corresponding to different lead times. There are significant correlations between the winter precipitation over LRYR and the SST in both the equatorial central and eastern Pacific and the equatorial Atlantic Oceans, which further confirms the significant relationship between these two regional factors and precipitation anomaly over LRYR in the observations (Fig. 3a). With the increase of the lead time, the prediction skill overall drops, likely due to the accumulation of

model biases and the decline of the ability in forecasting the SSTAs in the tropical Pacific and Atlantic Oceans. Therefore, it is not surprising that the predicted precipitation anomalies are opposite to the observed ones at the 7-month lead (Fig. 9d) though the relationship between the winter precipitation in LRYR and SST has little change with the increase of lead time (Fig. 11). Nevertheless, the skill does not decrease linearly with lead-time increase in some regions. For example, in the tropical central Pacific, the skill is higher for 7-month lead (Fig. 12d) than for 5-month lead (Fig. 12c), and higher for 3-month lead (Fig. 12b) than for 1-month lead (Fig.12a). In addition to feature of CFSv2, skill variation with lead time increase may be due to smapling.

5. Summary and discussion

In the winter of 2018/19, the LRYR of China experienced an excessive amount of precipitation with a long duration. Such an extreme event occurred during the mature phase of an El Niño event under the background of global warming, and thus, attracted great attention in the society and climate community. It has been well recognized that ENSO is a leading factor affecting the winter precipitation anomaly in South China. Thus, the community assumed that this extreme event was driven by ENSO (e.g. Guo et al., 2019). In this work, we investigate possible reasons and predictability of the extremely wet winter of 2018/19 in LRYR, in particular, the roles of the warming in the central tropical Pacific and equatorial Atlantic Oceans.

Our results show that in addition to the warming in the central tropical Pacific

associated with CP El Niño instead of EP El Niño, the warming in the equatorial Atlantic Ocean is another factor leading to the wet winter in LRYR in 2018/19 through generating a zonal wave train from the tropical Atlantic Ocean to East Asia. It is concluded that the warming in the central tropical Pacific and equatorial Atlantic Oceans plus interdecadal variation are three major factors causing the extreme event. The connections with SSTA imply the predictability of the event. That is confirmed by the success of the real-time forecasts of CFSv2 in short leads (1-5 months). Furthermore, the relationship between the winter precipitation in LRYR and the SSTA in the central tropical Pacific and equatorial Atlantic Oceans in the model is consistent with that in the observations.

The results suggest a potential source of the predictability of this extreme event. However, it should be pointed out that although the reconstruction of the three factors well reproduced the spatial distribution of the extremely wet winter in 2018/19, it underestimates the amplitudes of the precipitation anomaly over LRYR (about 1/4 of the observation), and overestimate the precipitation over southeastern coast of China (Figure not shown). The model predictions have similar results (Fig. 9). The discrepancy from the observations may be associated with the impact of internal dynamics driven processes, which are profound in the extra-tropics (such as, eastern China) and unpredictable (Gao et al. 2014; Liang et al. 2019; Liu et al., 2014, 2019).

Acknowledgments:

We thank three anonymous reviewers for their constructive connments and insightful

suggestions. For data used in this study, please contact us via liuyuny@cma.gov.cn. This work was jointly supported by the National Key R&D Program of China (2018YFC1505806, 2018YFB1502803) and National Natural Science Foundation of China (41730964). The forecast data of CFSv2 at NCEP/CPC were archived and maintained by Dr. Wanqiu Wang.

Reference

Alexander M, Blade I, Newman M, Lanzante J, Lau N-C, Scott J 2002 The atmospheric bridge: the influence of ENSO teleconnection on air-sea interaction over the global oceans. J Clim 15: 2205-2231.

Ashok K, Behera S K, Rao S A, Weng H, Yamagata T 2007 El Niño Modoki and its possible teleconnection. J Geophys Res 112: C11007, doi: 10.1029/2006JC003798.

Chambers D P, Tapley B D, Stewart R H 1999 Anomalous warming in the Indian Ocean coincident with El Niño. J Geophys Res 104: 3035–3047.

Chang C P, Wang Z, Ju J H, Li T 2004 On the relationship between western maritime continent monsoon rainfall and ENSO during northern winter. J Clim 17: 665-672, doi: 10.1175/1520-0442(2004)017<0665:OTRBWM>2.0.CO;2.

Chen, M., P. Xie, J. E. Janowiak, and P. A. Arkin, 2002: Global Land Precipitation: A 50-yr Monthly Analysis Based on Gauge Observations, 2002, J. Hydrometeorology, 3, 249-266.

Czaja A, and Frankignoul C 2002 Observed impact of Atlantic SST anomalies on the North Atlantic Oscillation. J Clim 15: 606 – 623.

Drevillon M, Cassou C, Terray L 2003 Model study of the North Atlantic region atmospheric response to autumn tropical Atlantic sea-surface-temperature anomalies. Q J R Meteorol Soc 129: 2591– 2611.

Enfield D B, Mestas A M, Mayer D A, Cid-Serrano L 1999 How ubiquitous is the dipole relationship in tropical Atlantic sea surface temperatures? J Geophys

Res 104: 7841-7848.

Feng J and Li J 2011 Influence of El Niño Modoki on spring rainfall over south China. J Geophys Res 116: D13102, doi: 10.1029/2010JD015160

Feng J, Wang L, Chen W, Fong S K, Leong K C 2010 Different impacts of two types of Pacific Ocean warming on Southeast Asian rainfall during boreal winter. J Geophys Res 115: D24122, doi: 10.1029/2010JD014761.

Fu J, Li S, Wang Y 2008 Influence of prior thermal state of global oceans on the formation of the disastrous snowstorm in January 2008. Clim Environ Res 13 (4): 478-490 (in Chinese).

Gao, Z, Hu Z-Z, Jha B, Yang S, Zhu J, Shen B, Zhang R 2014 Variability and predictability of Northeast China climate during 1948-2012. Clim Dyn 43 (3-4): 787-804, doi: 10.1007/s00382-013-1944-0.

Gill A 1980 Some simple solutions for heating-induced tropical circulation. Q J R Meteorol S 106: 447-462.

Guo L, Liu B, Zhu C. 2019. Extraordinary long wet spell in south of Yangtze River during 2018/2019 winter and its possible causes. Chin Sci Bull, 2019, 64: 3498–3509, doi: 10.1360/N972019-00357. (in Chinese).

Guo Y, Ni Y 1998 Effects of the tropical Pacific convective activities on China's winter monsoon. Meteorology 24 (9): 3-7 (in Chinese).

Han Z, Li S, Mu M 2011 The role of warm North Atlantic SST in the formation of position of positive height anomalies over the Ural Mountains during January 2008. Adv Atmos Sci 28 (2): 246-256.

He S, Wang H J 2013 Oscillating relationship between the East Asian winter monsoon and ENSO. J Clim 26: 9819-9838, doi: 10.1175/jcli-d-13-00174.1.

Hoerling M, Ting M, Blackmon M 1992 Simulating the atmospheric response to the 1985-87 El Nino Cycle. J Clim 5: 669-682.

Hu K M, Huang G, Wu R G, Wang L 2018 Structure and dynamics of a wave train along the wintertime Asian jet and its impact on East Asian climate. Clim Dyn 51: 4123-4137.

Hu Z-Z, Kumar A, Jha B, Wang W, Huang B H, and Huang B Y 2012 An analysis of warm pool and cold tongue El Niños: Air-sea coupling processes, global influences, and recent trends. Clim Dyn 38: 2017-2035, doi: 10.1007/s00382-011-1224-9.

Hu Z-Z, Kumar A, Huang B H, Wang W Q, Zhu J S, Wen C 2013 Prediction skill of monthly SST in the North Atlantic Ocean in NCEP Climate Forecast System version 2. Clim Dyn 40: 2745-2756, doi:10.1007/s00382-012-1431-z.

Hu Z-Z, Kumar A, Huang B H, Zhu J S, Guan Y 2014 Prediction skill of North Pacific variability in NCEP Climate Forecast System Version 2: Impact of ENSO and beyond. J Clim 27: 4263-4272, doi: 10.1175/JCLI-D-13-00633.1.

Hu Z-Z, Kumar A, Jha B, Zhu J S, Huang B H 2017 Persistence and predictions of the remarkable warm anomaly in the northeastern Pacific Ocean during 2014-2016. J Clim 30: 689–702, doi: 10.1175/JCLI-D-16-0348.1.

Hu, Z.-Z., A. Kumar, B. Jha, and B. Huang, 2020: How much of monthly mean precipitation variability over global land is associated with SST anomalies?

Clim Dyn 54 (1-2): 701-712. doi: 10.1007/s00382-019-05023-5.

Huang B, Thorne P W, Banzon V F, Boyer T, Zhang H M 2017 Extended Reconstructed Sea Surface Temperature version 5 (ERSSTv5), Upgrades, validations, and intercomparisons. J Clim 30: 8179-8205, doi: 10.1175/JCLI-D-16-0836.1.

Huang W, Yang Z, He X, Lin D, Wang B, Wright J S, Chen R, Ma W, Li F 2019 A possible mechanism for the occurrence of wintertime extreme precipitation events over South China. Clim Dyn 52: 2367-2384.

Kalnay E, Kanamitsu M, Kistler R, et al 1996 The NCEP/NCAR 40-Year Reanalysis Project. Bull Amer Meteor Soc 77: 437-472.

Kimoto M 2005 Simulated change of the East Asian circulation under global warming scenario. Geophy Res Lett 32(16): L16701, doi: 10.1029/2005GL023383.

Kug J S, Jin F F, An S I 2009 Two types of El Niño events: cold tongue El Niño and warm pool El Niño. J Clim 22: 1499-1515, doi: 10.1175/2008jcli2624.1.

Kumar A, Hoerling M P 1997 Interpretation and implication of the observed inter-El Nino variability. J Clim 10: 83-91.

Lau N-C and Nath M J 2003 Atmosphere-Ocean variations in the Indo-Pacific sector during ENSO episodes. J Clim 16: 3-20, doi: 10.1175/15200442(2003)016<0003: AOVITI>2.0.CO;2.

Li S, Bates G T 2007 Influence of the Atlantic multi-decadal oscillation on the winter climate of East China. Adv Atmos Sci 24 (1): 126-135.

Liang P, Hu Z-Z, Liu Y, Yuan X, Li X, Jiang X 2019 Challenges in predicting and

simulating summer rainfall in the eastern China. Clim Dyn 52 (3-4): 2217-2233, doi: 10.1007/s00382-018-4256-6.

Liu G, Zhao P, Dong C 2013 The relationship between the Asian-Pacific oscillation and January precipitation anomalies over southern China. Acta Meteor Sinica 71 (3): 462-475.

Liu S, Bueh C, Tao S, Sui B 2010 A study of the statistical prediction method of the East Asian winter monsoon intensity. Chin J Atmos Sci, 34 (1): 35-44 (in Chinese).

Liu Y, Ding Y 2012 Analysis of the leading modes of the Asian-Pacific summer monsoon system. Chin J Atmos Sci 36: 673–685 (in Chinese).

Liu Y, Ding Y, Gao H, Li W 2013 Tropospheric biennial oscillation of the western Pacific subtropical high and its relationships with the tropical SST and atmospheric circulation anomalies. Chin Sci Bull 58: 3664–3672, doi: 10.1007/s11434-013-5854-7.

Liu Y, Li W, Zuo J, Hu Z-Z 2014 Simulation and projection of western Pacific subtropical high in CMIP5 models. J Meteor Res 28(3): 327–340, doi: 10.1007/s13351-014-3151-2.

Liu Y, Hu Z-Z, Kumar A, Peng P, Collins D and Jha B 2015 Tropospheric biennial oscillation of summer monsoon rainfall over East Asia and its association with ENSO. Clim Dyn 45 (7–8): 1747–1759, doi: 10.1007/s00382-014-2429-5.

Liu Y, Ke Z, Ding Y 2019 Predictability of East Asian summer monsoon in seasonal climate forecast models. Int J Climatol 1–14, doi: 10.1002/joc.6180.

Mathieu P-P, Sutton R T, Dong B-W, Collins M 2004 The predictability of winter climate over the North Atlantic European region during ENSO events. J Clim 17: 1953–1974.

Nitta T, Hu Z-Z 1996 Summer climate variability in China and its association with 500 hPa height and tropical convection. J Meteor Soc Japan 74 (4): 425-445, doi: 10.2151/jmsj1965.74.4_425.

Peng P, Kumar A, Chen M, Hu Z-Z, Jha B 2019 Was the North American extreme climate in winter 2013/14 a SST forced response? Clim Dyn 52: 3099-3110, doi: 10.1007/s00382-018-4314-0.

Peng P, Kumar A, Hu Z-Z 2018 What drove Pacific and North America climate anomalies in winter 2014/15? Clim Dyn 51: 2667-2679, doi: 10.1007/s00382-017-4035-9.

Plumb R A 1985 On the three-dimensional propagation of stationary waves. J Atmos Sci 42(3): 217–229, doi: 10.1175/1520-0469(1985)0420217: OTTDP O2.0.CO;2.

Qian Z L 2013 Analysis of winter rainfall variability and influencing factors in the middle-lower reaches of Yangtze River. Plateau Meteor 32: 1795-1802 (in Chinese).

Ren H and Jin F-F 2011 Niño indices for two types of ENSO. Geophys Res Lett 38: L04704, doi: 10.1029/2010GL046031.

Saha S et al 2014 The NCEP Climate Forecast System version 2. J Clim 27: 2185–2208, doi: 10.1175/JCLI-D-12-00823.1.

Saji N H, Goswami B N, Vinayachandran P N, Yamagata T 1999 A dipole mode in the tropical Indian Ocean. Nature 401: 360–363, doi: 10.1038/43854.

Sardeshmukh PD, Hoskins BJ 1988 Generation of global rotational flow by steady idealized tropical divergence. J Atmos Sci 45(7): 1228-1251.

Shi X, Xu X, Xie L 2007 Interdecadal spatial-temporal change trend of East Asian winter monsoon in the Last 40 years. Chin Atmos Sci 31(4): 747-756. (in Chinese).

Su J Z, Zhang R H, Zhu C W 2013 ECHAM5-simulated impacts of two types of El Niño on the winter precipitation anomalies in South China. Atmos Oceanic Sci Lett 6: 360-364, doi: 10.3878/j.issn.1674-2834.13.0013.

Takaya K, Nakamura H 2005 Geographical dependence of upperlevelblocking formation associated with intraseasonal amplification of the Siberian high. J Atmos Sci 62 (12): 4441–4449, doi: 10.1175/JAS36 28.1.

Tam CY, Li T 2006 The origin and dispersion characteristics of the observed tropical summertime synoptic-scale waves over theWestern Pacific. Mon Wea Rev 134(6): 1630–1646, doi: 10.1175/MWR31 47.1.

Tao S 1998 Response of the Asian winter and summer monsoon to ENSO events. Scientia Atmos Sinica 22(4): 399-407.

Ting M, Hoerling M 1993 Dynamics of stationary wave anomalies during the 1986/87 El Nino. Clim Dyn 9: 147-164.

Wallace M, Blackmon M 1983 Observations of low-frequency atmospheric variability. Large-Scale Dyn Proc Atmos. Academic Press, p397.

Wang B, Wu R G, Fu X H 2000 Pacific-East Asian teleconnection: How does ENSO affect East Asian climate? J Clim 13: 1517-1536, doi: 10.1175/1520-0442(2000)013<1517:PEATHD>2.0.CO;2.

Wang H 2001 The weakening of the Asian monsoon circulation after the end of 1970s. Adv Atmos Sci 18(3): 376-386.

Wang L, Chen W 2014 An intensity index for the East Asian winter monsoon. J Clim 27: 2361-2374, doi: 10.1175/jcli-d-13-00086.1.

Wu R G, Hu Z-Z, Kirtman B P 2003 Evolution of ENSO-related rainfall anomalies in East Asia. J Clim 16: 3742-3758, doi: 10.1175/1520-0442(2003)016<3742:EOERAI>2.0.CO;2.

Xie S P, Hu K, Hafner J, Tokinaga H, Du Y, Huang G, Sampe T 2009 Indian Ocean capacitor effect on Indo-Western Pacific climate during the summer following El Niño. J Clim 22: 730-747, doi: 10.1175/2008jcli2544.1.

Xu K, Huang Q L, Tam C Y, Wang W Q, Chen S, Zhu C W 2019 Roles of tropical SST patterns during two types of ENSO in modulating wintertime rainfall over southern China. Clim Dyn 52: 523-538, doi: 10.1007/s00382-018-4170-y.

Xue Y, Chen M, Kumar A, Hu Z-Z, Wang W 2013 Prediction skill and bias of tropical Pacific sea surface temperatures in the NCEP Climate Forecast System version 2. J Clim 26: 5358-5378, doi: 10.1175/JCLI-D-12-00600.1.

Yuan Y and Yang S 2012 Impacts of different types of El Niño on the East Asian climate: Focus on ENSO cycles. J Clim 25: 7702-7722.

Yuan Y, Li C Y, Yang S 2014 Decadal anomalies of winter precipitation over southern

China in association with El Niño and La Niña. J Meteorol Res 28(1): 91–110. doi: 10.1007/s13351-014-0106-6.

Zebiak S E 1993 Air-sea interaction in the equatorial Atlantic region. J Clim 6: 1567–1586, doi: 10.1175/1520-0442(1993)006<1567:AIITEA>2.0.CO;2.

Zhang F Y，Pan A J，Fan L L 2018 Interdecadal differences in correlations between the winter precipitation over the southern China and El Niño events and their cause. J Marine Meteor 38: 38-44 (in Chinese).

Zhang R H, Sumi A, Kimoto M 1996 Impact of El Niño on the East Asian monsoon: a diagnostic study of the 86/87 and 91/92 events. J Meteor Soc Japan 74: 49-62.

Zhang R H, Sumi A, Kimoto M 1999 A diagnostic study of the impact of El Niño on the precipitation in China. Adv Atmos Sci 16: 229-241.

Zhang R H and Sumi A 2002 Moisture circulation over East Asia during El Niño episode in the northern winter, spring and autumn. J Meteor Soc Japan 80: 213-227.

Zhang Z, Gong D, Guo D, He X, Lei Y 2008 Anomalous winter temperature and precipitation events in southern China. Acta Geograph Sinica, 63 (9): 899-912 (in Chinese).

Zhou L, Wu R 2010 Respective impacts of the East Asian winter monsoon and ENSO on winter rainfall in China. J Geophys Res, 115, D0217, doi: 10.1029/2009JD012502.

Zhou L 2011 Impact of East Asian winter monsoon on rainfall over southeastern China and its dynamical process. Inter J Climatol 31(5): 677-686.

Zong H, Zhang Q, Bueh C, Ji L, Chen L 2008 Numerical simulation of possible impacts of Kuroshio and North Atlantic sea surface temperature anomalies on the South China snow disaster in January 2008. Clim Environ Res 13 (4): 491-499 (in Chinese).

Table Caption

Table 1: Simultaneous correlation coefficients of precipitation anomaly in LRYR (Pr_{LRYR}, Fig. 2) with various tropical SST indices and among the SST indices during DJF 1951/52-2018/19 after the linear trends have been removed. Thick numbers are significant at the 99% significance level using Student's *t*-test, corresponding to the absolute value of correlation ≥ 0.31

Figure Captions

Fig. 1: (a) Precipitation (mm) and (b) the number of precipitation day anomalies (shading) and normalized anomalies (contour) in DJF 2018/19. The blue rectangle denotes southern China (SC), and the red rectangle represents the lower reach of the Yangtze River (LRYR).

Fig. 2: The time series of DJF ATL3 index (left axis, green bars, °C) and precipitation anomaly averaged in LRYR (27°-33°N, 112°-123°E) (right axis, blue bars, mm) during 1951/52-2018/19.

Fig. 3: (a) SST (shading, °C) and 200hPa geopotential height (contour, gpm) anomalies; (b) 200hPa eddy stream function (contour, interval: 3×0^6 m^2s^{-1}) and precipitation (shading, mm), and wave activity flux (vectors, m^2s^{-2}) anomalies in DJF 2018/19

Fig. 4: Simultaneous correlations between precipitation anomaly and the de-trended SST indices of (a) Niño3.4; (b) CT; (c) WP; (d) Modoki; (e) IOBM; (f) IOD; (g) ATL3; (h) TNA during DJF 1951/52 -2018/19. The red dots indicate correlation coefficients reaching the 95% confidence level according to Student's *t*-test.

Fig. 5: Reconstructions of 2018/19 DJF precipitation anomaly (mm) based on the linear regression with the de-trended (a) WP and (b) ATL3 indices; (c) the interdecadal change of the DJF precipitation (mm) in 1989/90-2018/19 and 1951/52-1988/89; (d) the sum of (a), (b) and (c).

Fig. 6: The moving *t*-test for the time series of winter precipitation anomaly in LRYR from 1951/ 1952 to 2018/2019 (the moving window is 10 years. The red dash lines denote the 95% significant levels).

Fig. 7: Composites of (a) SST (shading, °C) and 200hPa geopotential height (contour, gpm) anomalies; (b) 200hPa eddy stream function (contour, interval: 2×0^6 m^2s^{-1}), precipitation (shading, mm), and wave activity flux (vectors, m^2s^{-2}) anomalies in typical positive and negative ATL3 winters.

Fig. 8: Correlations of the observed and CFSv2 predicted DJF precipitation anomalies with initial conditions in (a) November, (b) September, (c) July, and (d) June during 1982-2010.

Fig. 9: CFSv2 real-time forecasts of precipitation anomalies (mm) in DJF 2018/19 in the (a) 1-month, (b) 3-month, (c) 5-month, and (d) 7-month leads.

Fig. 10: CFSv2 predicted DJF precipitation anomalies in 1983/84~2018/19 averaged in the LRYR (27°-33°N, 112°-123°E) in the (a) 1-month; (b) 3-month, (c) 5-month, and (d) 7-month leads. The dished lines represents one positive and negative standard deviation. The unit is mm.

Fig.11: CFSv2 real-time forecasts of SST anomalies (°C) in DJF 2018/19 in the (a) 1-month, (b) 3-month, (c) 5-month, and (d) 7-month leads.

Fig. 12: Simultaneous correlations between the LRYR precipitation anomaly and SSTA in the (a) 1-month, (b) 3-month, (c) 5-month, and (d) 7-month leads in CFSv2 predictions in January 1982 – December 2018. The cross signs indicate correlation coefficients reaching the 95% significant level according to Student's *t*-test.

Table 1: Simultaneous correlation coefficients of precipitation anomaly in LRYR (Pr_{LRYR}, Fig. 2) with various tropical SST indices and among the SST indices during DJF 1951/52-2018/19 after the linear trends have been removed. Thick numbers are significant at the 99% significance level using Student's *t*-test, corresponding to the absolute value of correlation ≥ 0.31

	Niño34	**CTP**	**WPoki**	**Modoki**	**IOBM**	**IOD**	**ATL3**	**TNA**
Pr_{LRYR}	**0.33**	0.30	**0.31**	0.29	**0.39**	002	**0.31**	-0.05
Niño34		**0.90**	**0.66**	**0.68**	**0.81**	-0.01	0.20	0.18
CTP			0.29	0.30	**0.75**	0.04	0.26	0.10
WP				**0.95**	**0.50**	-0.05	0.06	0.25
Modoki					**0.48**	-0.08	0.01	0.20
IOBM						0.02	**0.31**	**0.33**
IOD							0.17	0.10

AT	0.15
L3	

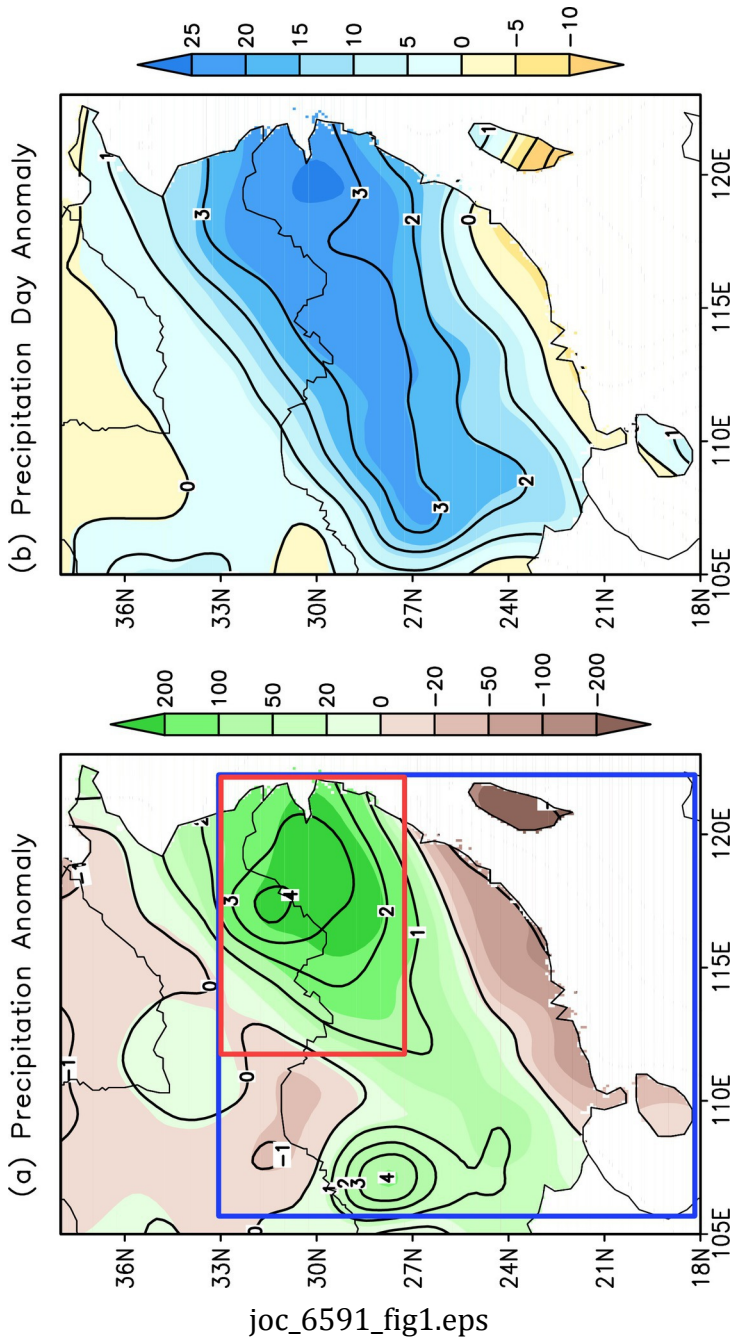

joc_6591_fig1.eps

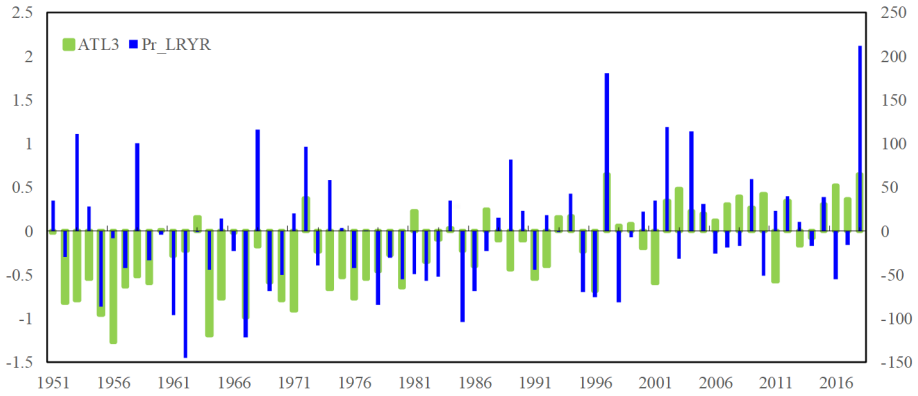

JOC_6591_Fig2.tif

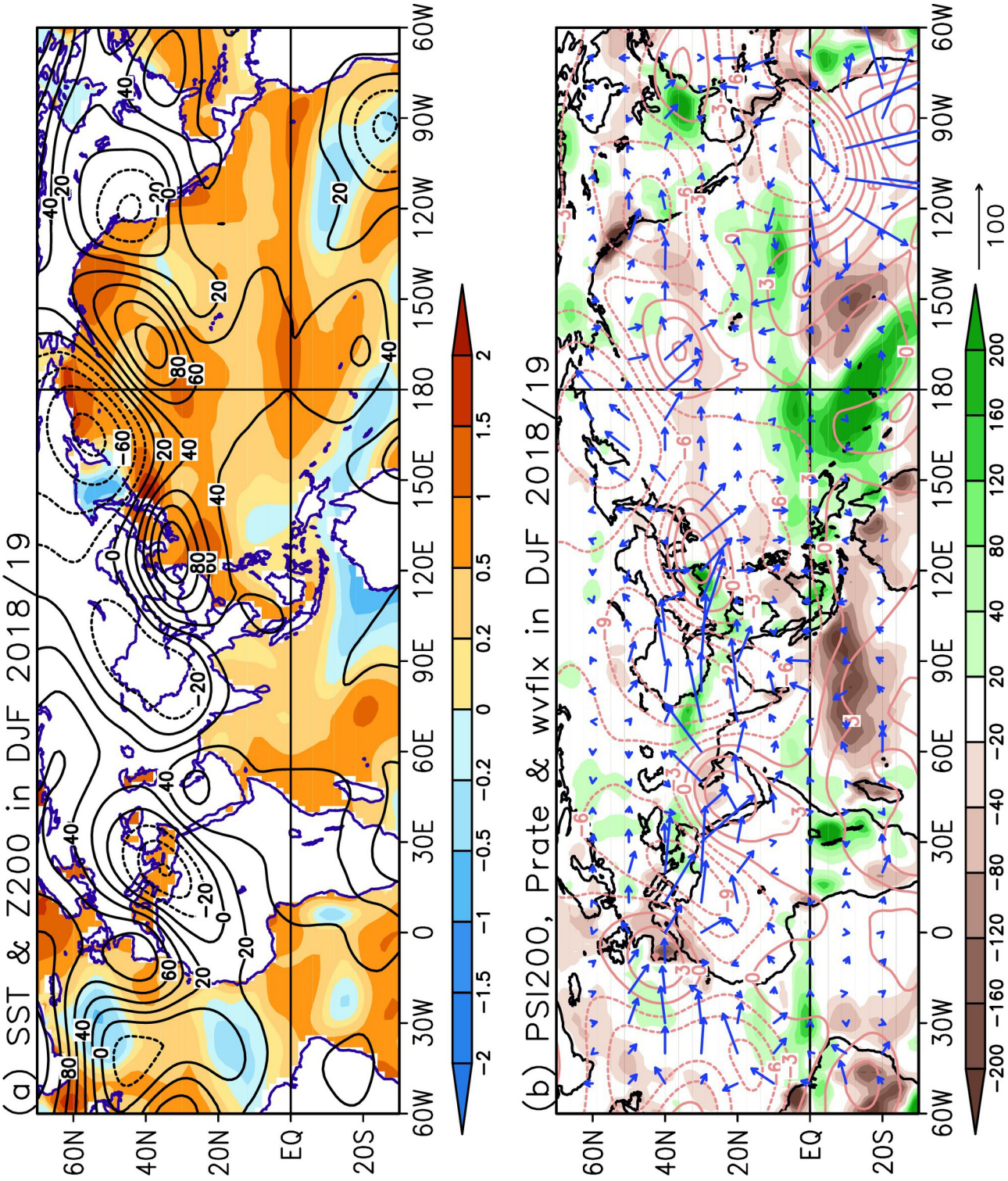

joc_6591_fig3.eps

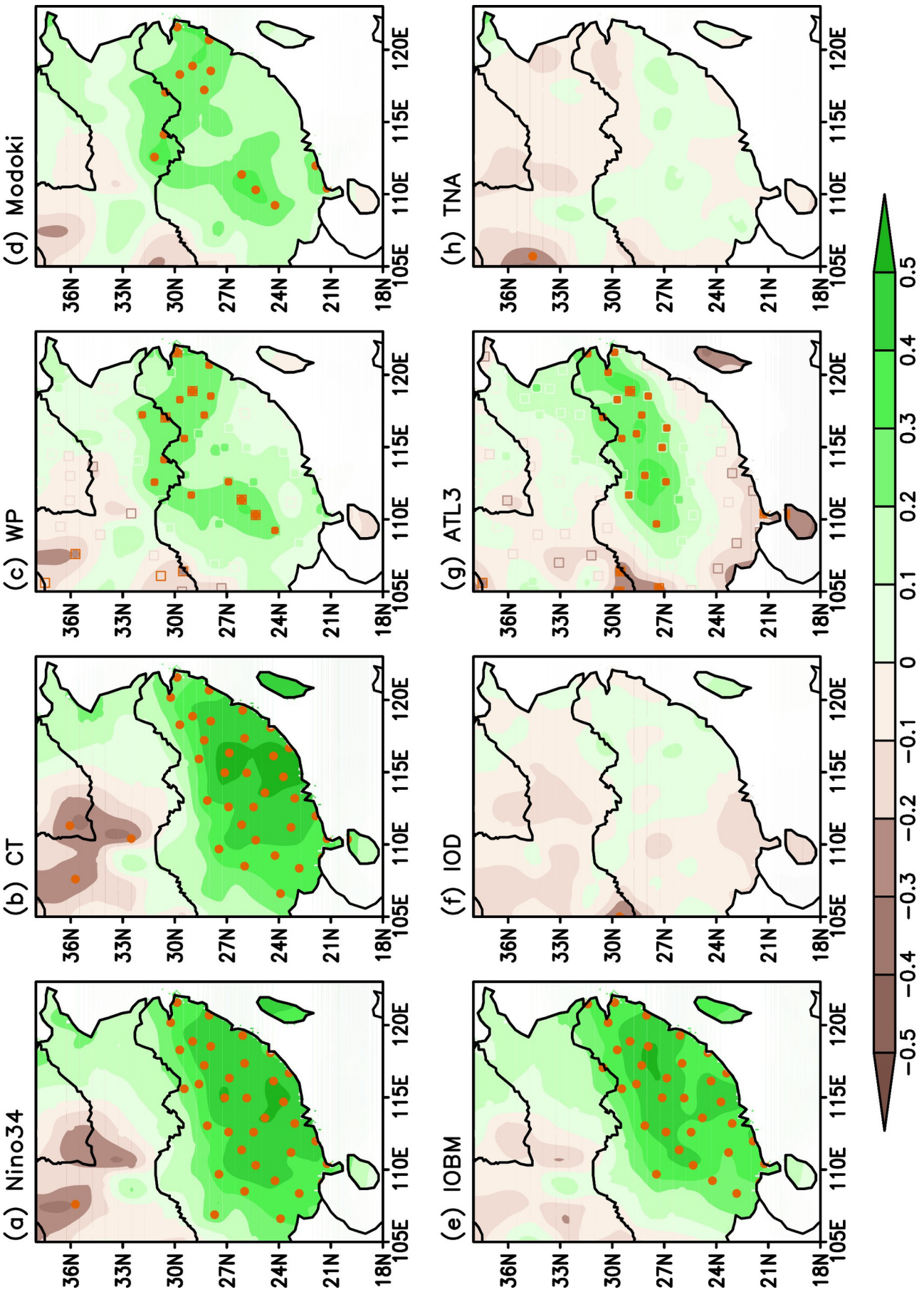

joc_6591_fig4.eps

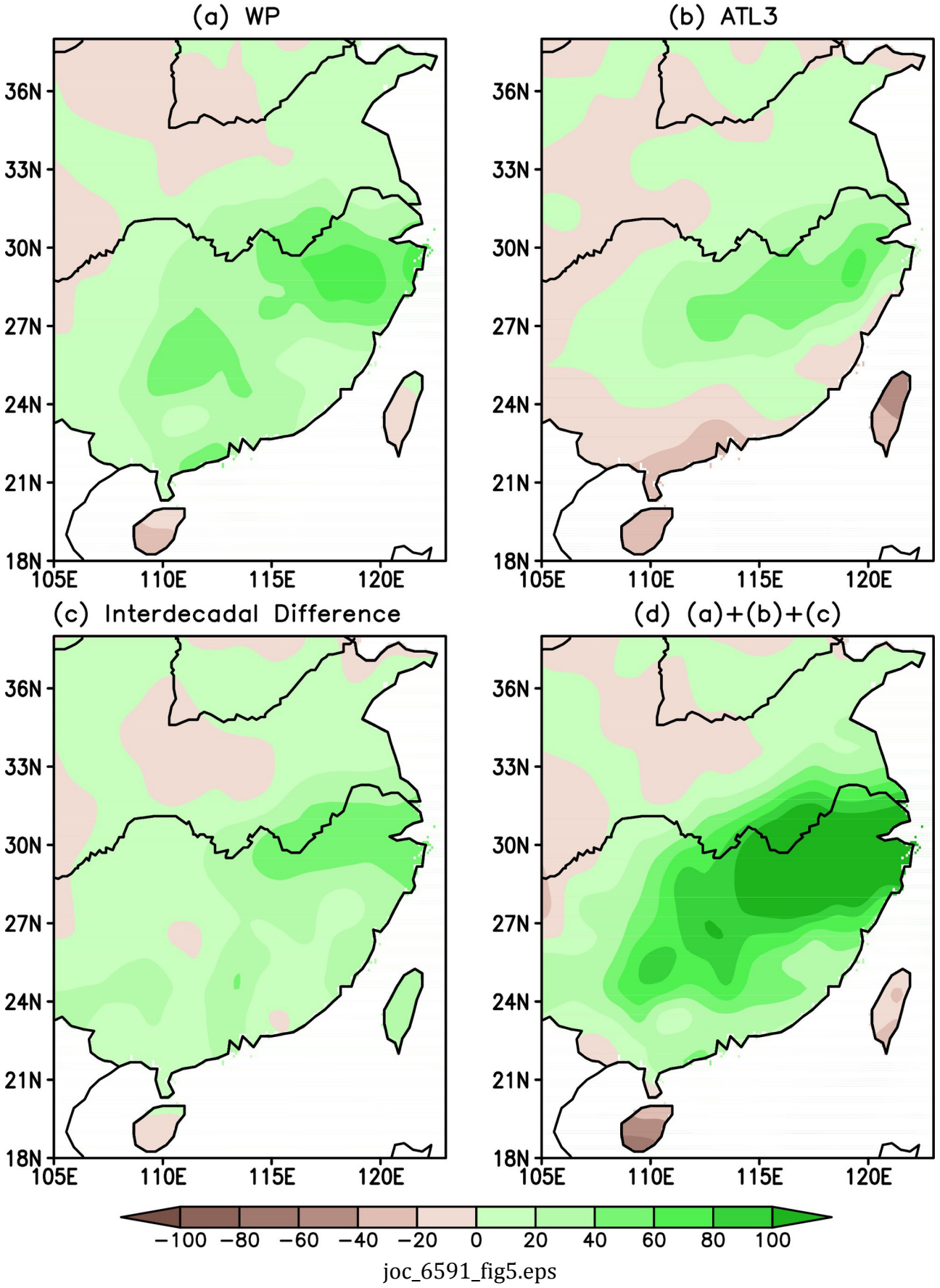

joc_6591_fig5.eps

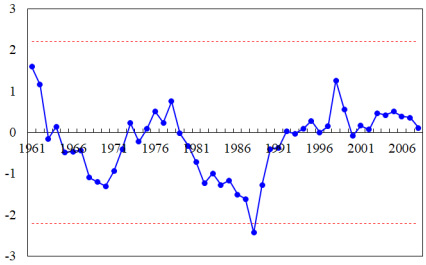

JOC_6591_Fig6.tif

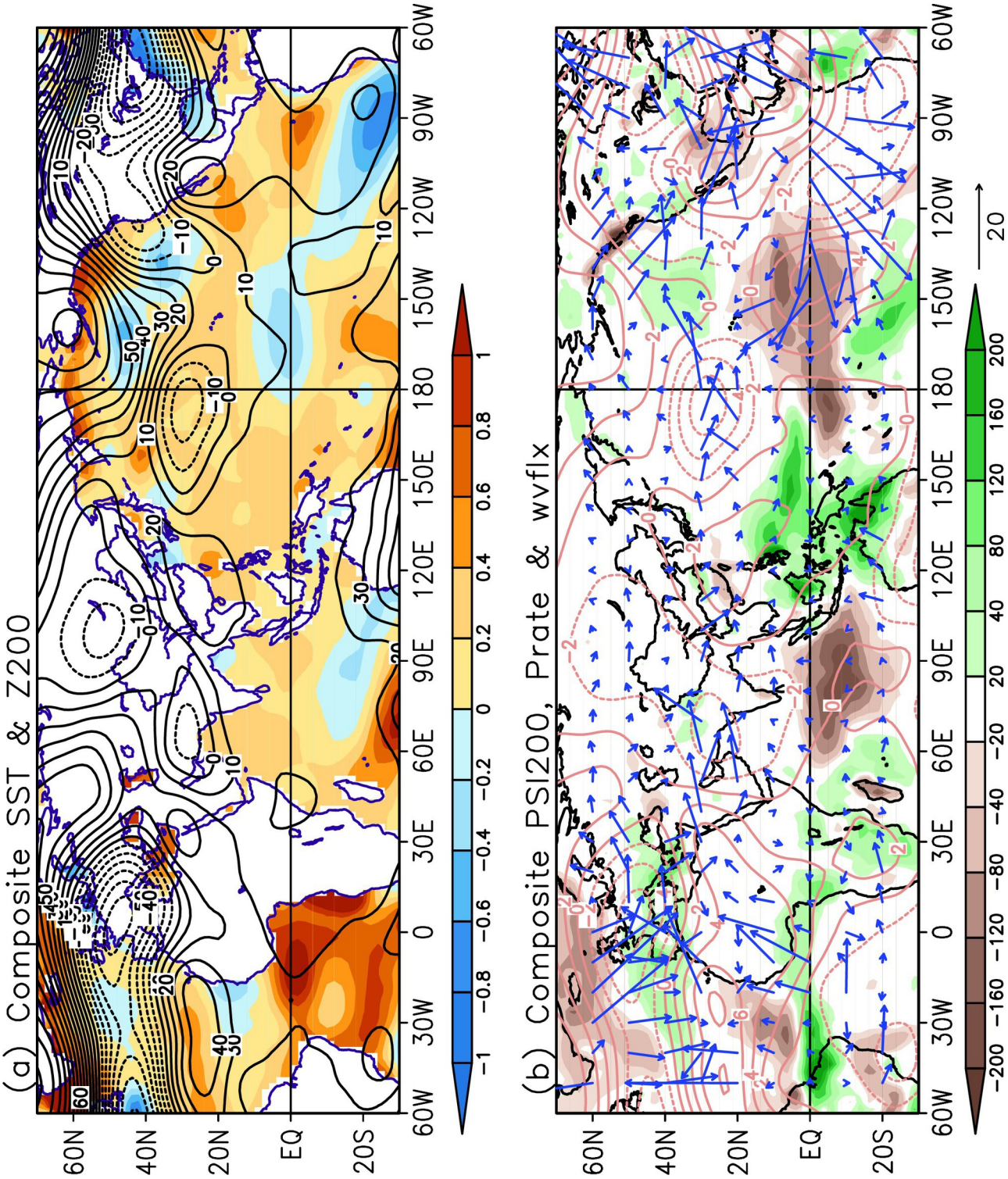

joc_6591_fig7.eps

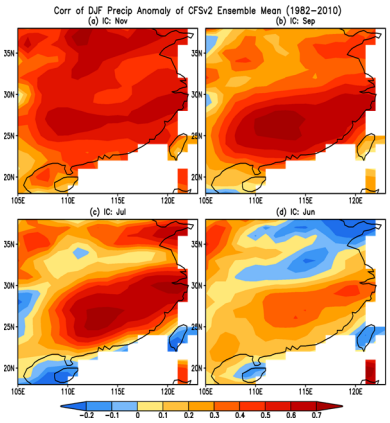

JOC_6591_Fig8.tif

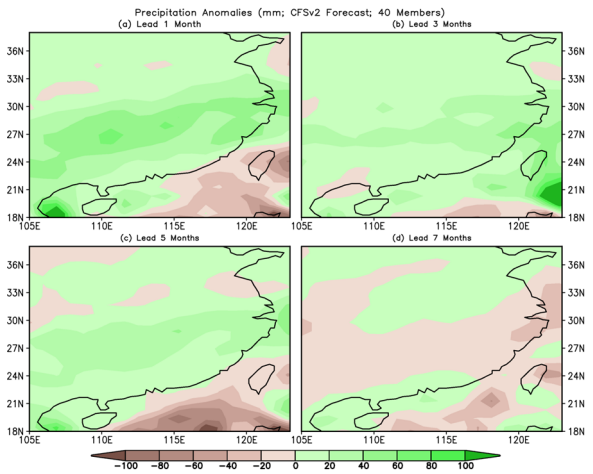

JOC_6591_Fig9.tif

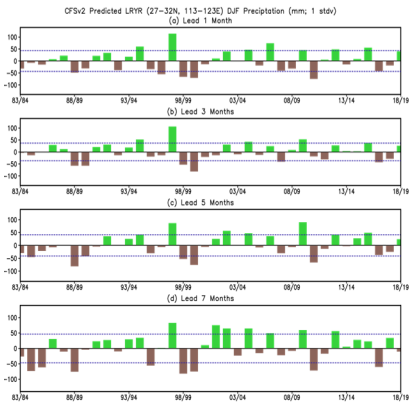

JOC_6591_Fig10.tif

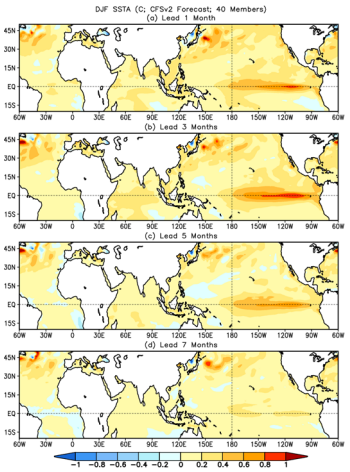

JOC_6591_Fig11.tif

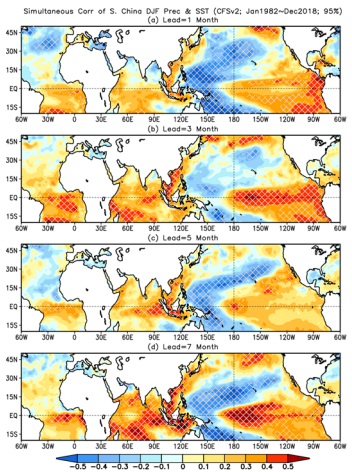

JOC_6591_Fig12.tif

Was the Extremely Wet Winter of 2018/19 in the Lower Reach of the Yangtze River Driven by ENSO?

Yunyun Liu[1, 2], Zeng-Zhen Hu[3], and Renguang Wu[4]

(1) Laboratory of Climate studies, National Climate Center, China Meteorological Administration, Beijing 100081, China

(2) Collaborative Innovation Center on Forecast and Evaluation of Meteorological Disasters, Nanjing University of Information Sciences & Technology, Nanjing 210044, China

(3) Climate Prediction Center, NCEP/NOAA, College Park, MD 20740, USA

(4) School of Earth Sciences, Zhejiang University, Hangzhou, Zhejiang 310027, China

Brief Summary

Tropical Atlantic warming, interdecadal variation, and central tropical Pacific warming (associated with central Pacific instead of eastern Pacific El Niño) are three major factors leading to the extremely wet winter of 2018/19 in the lower reach of the Yangtze River (LRYR). The real-time prediction results of successfully captured the observed statistical relationship between the winter precipitation in LRYR and the SSTA in the central tropical Pacific and equatorial Atlantic Oceans indicates that such an event is predictable to some extent.

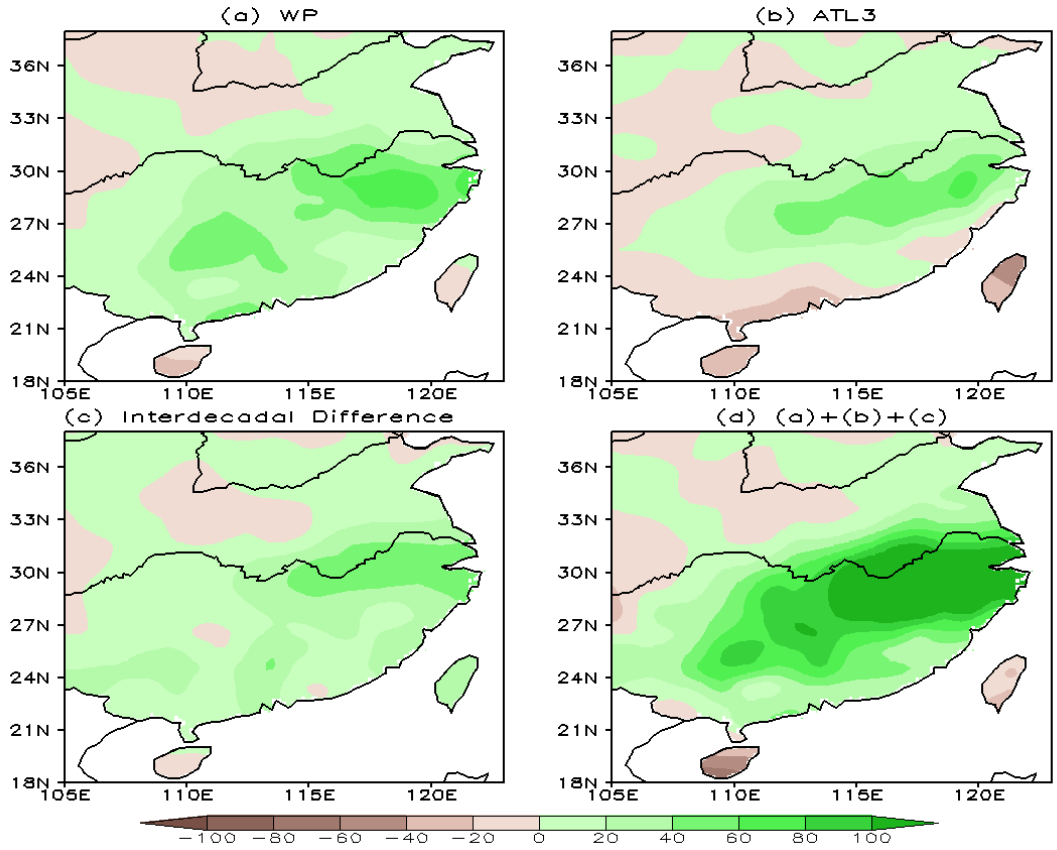

Fig. 1: Reconstructions of 2018/19 DJF precipitation anomaly based on the linear regression with the de-trended (a) WP and (b) ATL3 indices; (c) the interdecadal change of the DJF precipitation in 1989/90-2018/19 and 1951/52-1988/89; (d) the sum of (a), (b) and (c).

Table 1: Simultaneous correlation coefficients of precipitation anomaly in LRYR (Pr_{LRYR}, Fig. 2) with various tropical SST indices and among the SST indices during DJF 1951/52-2018/19 after the linear trends have been removed. Thick numbers are significant at the 99% significance level using Student's *t*-test, corresponding to the absolute value of correlation ≥ 0.31

	Nino34	**CT**	**WP**	**Modoki**	**IOBM**	**IOD**	**ATL3**	**TNA**
Pr_{LRYR}	**0.33**	0.30	**0.31**	0.29	**0.39**	002	**0.31**	-0.05
Niño34		**0.90**	**0.66**	**0.68**	**0.81**	-0.01	0.20	0.18
CT			0.29	0.30	**0.75**	0.04	0.26	0.10
WP				**0.95**	**0.50**	-0.05	0.06	0.25
Modoki					**0.48**	-0.08	0.01	0.20
IOBM						0.02	**0.31**	**0.33**
IOD							0.17	0.10
ATL3								0.15